Electronic Supplementary Material (ESI) for ChemComm.

Supporting Information

Pt(II)-Catalyzed Photosynthesis for H_2 Evolution Cycling Between Singly and Triply Reduced Species

Keiya Yamamoto,[a] Kyoji Kitamoto,[a,b] Kosei Yamauchi,[a,b] and Ken Sakai*[a,b,c]

[a]*Department of Chemistry, Faculty of Sciences, Kyushu University, 6-10-1 Hakozaki, Higashi-ku, Fukuoka 812-8581, Japan.*

[b]*International Institute for Carbon-Neutral Energy Research (WPI-I2CNER), Kyushu University, 744 Moto-oka, Nishi-ku, Fukuoka 819-0395, Japan.*

[c]*Center for Molecular Systems (CMS), Kyushu University, 744 Moto-oka Nishi-ku, Fukuoka 819-0395, Japan.*

*E-mail: ksakai@chem.kyushu-univ.jp

Experimental Section

Materials

N,N'-Dicyclohexylcarbodiimide (DCC), N-hydroxysuccinimide (NHS), and N,N'-dimethyl-4-aminopyridine (DMAP) were purchased from Watanabe Chemical Industries. All other chemicals and solvents were purchased from Kanto Chemicals Co., Inc. and used without further purification. 4,4'-Dicarboxy-2,2'-bipyridine (dcbpy),[S1] 1-(2-aminoethyl)-1'-methyl-4,4'-bipyridinium hexafluorophosphate,[S2] *cis*-$PtCl_2(DMSO)_2$ (DMSO = dimethylsulfoxide),[S3] $PtCl_2$(dcbpy)[S4] and $[Ru(bpy)_3](NO_3)_2 \cdot 3H_2O$[S5] were synthesized as previously described.

General Methods

UV-Vis and UV-Vis-NIR spectra were recorded on a Shimadzu UV-2600 and a Shimadzu UV-3600 spectrophotometer, respectively. Luminescence spectra were recorded on a Shimadzu RF5300PC spectrofluorophotometer. Low temperature emission spectra were measured for the glassy 77-K solution of each system contained in a quartz EPR tube. Emission decays were recorded on a HORIBA FluoroCube 3000USKU. The excitation source was a diode laser (374 nm) (HORIBA N-375L). ^{1}H NMR spectra were acquired on a JEOL JNM-ESA 600 spectrometer. Square wave voltammograms were recorded on a BAS ALS Model 602DKM electrochemical analyzer, using a three electrode system consisting of a platinum working electrode, a platinum wire counter electrode, and a Ag/Ag^+ reference electrode (0.249 V vs. SCE), where TBAP (tetra(n-butyl)ammonium perchlorate) was used as a supporting electrolyte and all potentials reported are given relative to the Fc/Fc^+ couple (Fc/Fc^+ = 0.155 vs SCE).

Synthesis of bpyMV2$(PF_6)_4 \cdot 2H_2O$

A solution of 4,4'-dicarboxy-2,2'-bipyridine (501 mg, 2.05 mmol) in dry DMF (N,N-dimethylformamide) (20 mL) was stirred in the presence of DCC (282 mg, 4.12 mmol) and NHS (475 mg, 4.13 mmol) at 40 °C for 15 h. Then, the reaction mixture was filtered for the removal of insoluble materials. Ethanol (20 mL) and hexane (60 mL) were added to the filtrate. The resulting white solid was collected by filtration and dried in vacuo (4,4'-dicarboxysuccinimidyl-2,2'-bipyridine, 605 mg, 67.3 %). 1-(2-Aminoethyl)-1'-methyl-4,4'-bipyridinium hexafluorophosphate (405 mg, 0.801 mmol) and DMAP (98.4 mg, 0.805 mmol) were dissolved in dry DMF (2 mL), and the solution was added into a solution of 4,4'-dicarboxysuccinimidyl-2,2'-bipyridine (162 mg, 0.368 mmol) in dry DMF (6 mL). The solution was stirred at 30 °C for 12 h. Then, the total volume of the solution was reduced to ca. 2 mL under reduced pressure, followed by addition of water (ca. 10 mL) to

give the product as a pale pink solid. The product was redissolved in a mixture of water (5 mL) and acetone (5 mL) at 50 °C. Then the solution was left in air overnight to promote gradual evaporation of acetone to re-precipitate the final product, which was collected and dried in vacuo (yield: 358 mg, 77.4 %). ^{1}H NMR (CD_3CN/TMS, ppm): δ 8.95 (d, *J* = 6.8 Hz, 4H), 8.83 (d, *J* = 6.9 Hz, 4H), 8.79 (d, *J* = 5.0 Hz, 2H), 8.69 (s, 2H), 8.38-8.35 (m, 8H), 7.67-7.62 (m, 4H), 4.83 (t, *J* = 5.6 Hz, 4H), 4.39 (s, 6H), 4.01 (m, 4H); Anal. Calcd for $C_{38}H_{42}F_{24}N_8O_4P_4 \bullet 2H_2O$ (1254.65): C, 36.38; H, 3.37; N, 8.93. Found: C, 36.39; H, 3.39; N, 9.03.

Synthesis of $[PtCl_2(bpyMV2)](PF_6)_4 \bullet 2H_2O$

This was prepared by refluxing a solution of *cis*-$PtCl_2(DMSO)_2$ (70.1 mg, 0.166 mmol) and **bpyMV2**$(PF_6)_4 \bullet 2H_2O$ (201 mg, 0.160 mmol) in methanol (30 mL) for 11 h. After cooling down to room temperature, the resulting yellow solid was collected by filtration and recrystallized from a water/acetone mixture as described above for **bpyMV2**$(PF_6)_4 \bullet 2H_2O$ (yield: 134 mg, 53.2 %). ^{1}H NMR (CD_3CN/TMS, ppm): δ 9.87 (d, *J* = 6.2 Hz, 2H), 8.95 (d, *J* = 6.9 Hz, 4H), 8.85 (d, *J* = 6.9 Hz, 4H), 8.57 (s, 2H), 8.40 (d, *J* = 6.8 Hz, 4H), 8.37 (d, *J* = 6.9 Hz, 4H), 7.85 (dd, *J* = 6.2, 1.6 Hz, 2H), 7.79 (s, 2H), 4.86 (t, *J* = 5.5 Hz, 4H), 4.40 (s, 6H), 4.03 (m, 4H); Anal. Calcd for $C_{38}H_{42}Cl_2F_{24}N_8O_4P_4Pt \bullet 2H_2O$ (1520.63): C, 30.01; H, 2.78; N, 7.37. Found: C, 30.01; H, 2.61; N, 7.36.

Photolysis Experiments

The photoirradiation was carried out by an ILC Technology CERMAX LX-300 Xe lamp (300 W) equipped with a CM-1 cold mirror ($400 < \lambda < 800$ nm). Photolysis was carried out using Pyrex glass vials which eliminates the lights below ca. 350 nm. Other experimental details are all same to those reported elsewhere.[S6]

DFT Calculations

Density functional theory (DFT) calculations were performed using the Gaussian 09 package of programs[S7] to better understand the structural and spin-state candidates for the π-dimers given by stacking of two singly reduced viologen moieties within the PHEMD reported herein. Calculations were also performed to simulate the UV-Vis-NIR absorption spectra of the candidates computed. The structures were fully optimized using the M06 hybrid functional, developed by Truhlar *et al.*[S8–S10] with the effect of solvation in water taken into consideration using the polarizable continuum model (PCM) method.[S11-S13] The SDD basis set was adopted for the Pt ion, while the 6-31G** basis set was applied to the rest of atoms. The choice of 6-31G** relies on our experience that calculations using the 6-31G** basis set afford results essentially identical to those calculated using the 6-311+G(2d,p) basis set when this type of

aromatic-aromatic interactions are computed using the M06 hybrid functional. Spin-restricted and -unrestricted methods (i.e., M06 and UM06) were respectively employed for closed- and open-shell singlet states. Particularly, UM06 calculations (Guess=Mix) in broken symmetry (BS) were performed for the open-shell singlet states. For such BS singlet-state calculations, spin contamination is exhibited by nonzero values for the spin-squared expectation value, defined with $<S^2> = S(S+1)$, where S is the molecular spin quantum number. Actually, the spin-squared expectation value after spin annihilation was confirmed to be 0.00, showing that spin contamination of the triplet state is negligible. This supports the validity of the BS approach for the open-shell singlet state without employing the spin-projected methods eliminating the redundant spin contaminations. Moreover, this open-shell singlet-state calculation afforded results equivalent to those given in the closed-shell singlet-state calculation (see below). All stationary points were characterized by their harmonic vibrational frequencies as minima. The unscaled frequencies were used to compute the zero-point vibrational energy corrections to the energies. Electronic excited states were calculated by the TD-DFT method as implemented in Gaussian 09[S14-S16] with use of the M06 functional and the same basis sets described above (Fig. S10). We also tested the used of other functionals such as CAM-B3LYP, PBE0, B3PW91, and M06-2X (see Fig. S10), showing that the selection of M06 functional is valid within the scope our study here. The calculated transitions were replaced by a Gaussian broadening function with a full width at half maximum height of 0.2 eV to simulate the electronic transition spectrum. Molecular orbital pictures were generated using GaussView 5.0.[S17]

Quantum Yield Determination

The quantum yield for the H_2 evolution from water photocatalyzed by **$[PtCl_2(bpyMV2)]^{4+}$** was determined using potassium ferrioxalate, $K_3[Fe(III)(C_2O_4)_3]$, as a chemical actinometer.[S18] The light source was same to that described above. However, the wavelength region used in the actinometry was further diminished into the range 360-400 nm (see Fig. S11) by employing a combination of Asahi Spectra SU400 and SV490 band-path glass filters. The chemical actinometry was carried out under the condition which satisfies complete absorption of lights within this wavelength range (see Fig. S11). The photon flux was determined as 5.22×10^{-7} einstein/s. The H_2 evolution rate under the steady state was determined as 2.677×10^{-11} mol/s (Fig. S12). As a result, the apparent quantum yield for H_2 evolution was determined as $\Phi(0.5H_2) = 0.010$. This value was further corrected into the more meaningful value which defines $\Phi(0.5H_2)$ on the basis of absorption at the MLCT band of the $PtCl_2$(bpy) chromophore. The correction factor was estimated as 0.53 (see Fig. S11) by evaluating the absorption features of both non-reduced and two-electron-reduced forms of **$[PtCl_2(bpyMV2)]^{4+}$**.

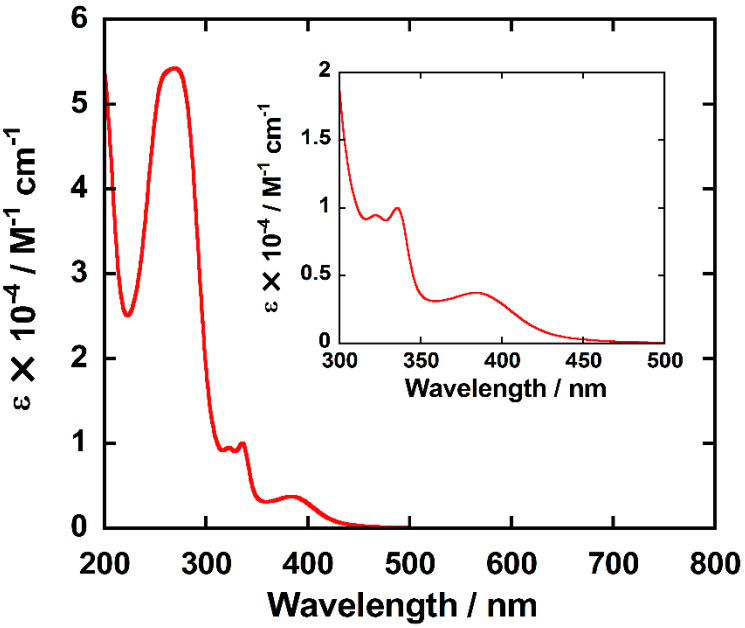

Fig. S1 An absorption spectrum of **[PtCl$_2$(bpyMV2)]$^{4+}$** in an aqueous 0.1 M NaCl solution at 20 °C in air. The inset shows a magnification in the range 300-500 nm. The molar absorptivities at 270, 336, and 387 nm have been determined as 54200, 10000, and 3700 M^{-1} cm^{-1}, respectively.

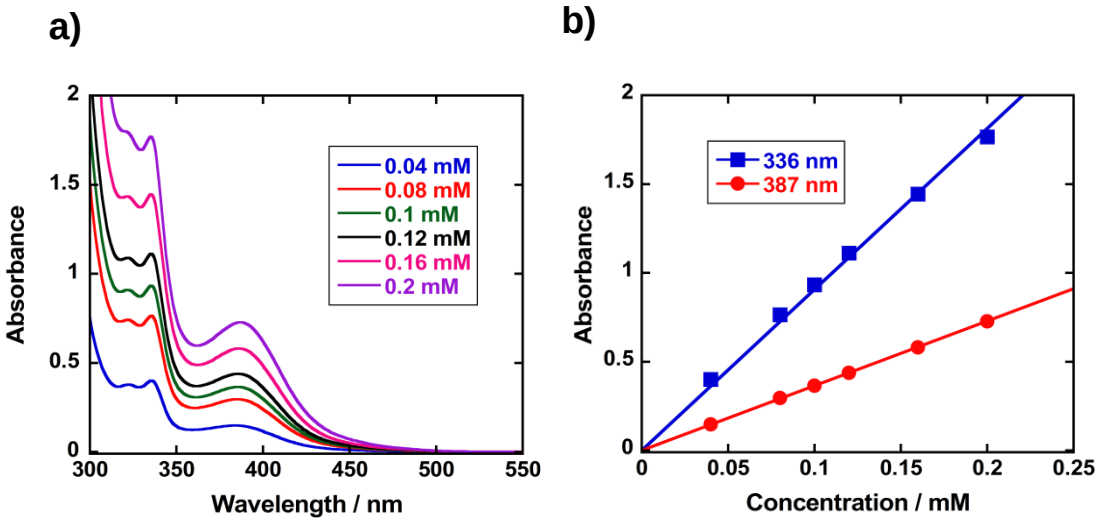

Fig. S2 a) UV-Vis absorption spectra of **[PtCl$_2$(bpyMV2)]$^{4+}$** in an aqueous 0.1 M NaCl solution at various concentrations, at 20 °C in air. b) The concentration dependences of absorbance at two wavelengths in the concentration range of 0.04-0.2 mM, showing that they obey Beer's law and is thereby dimerization in solution is negligible.

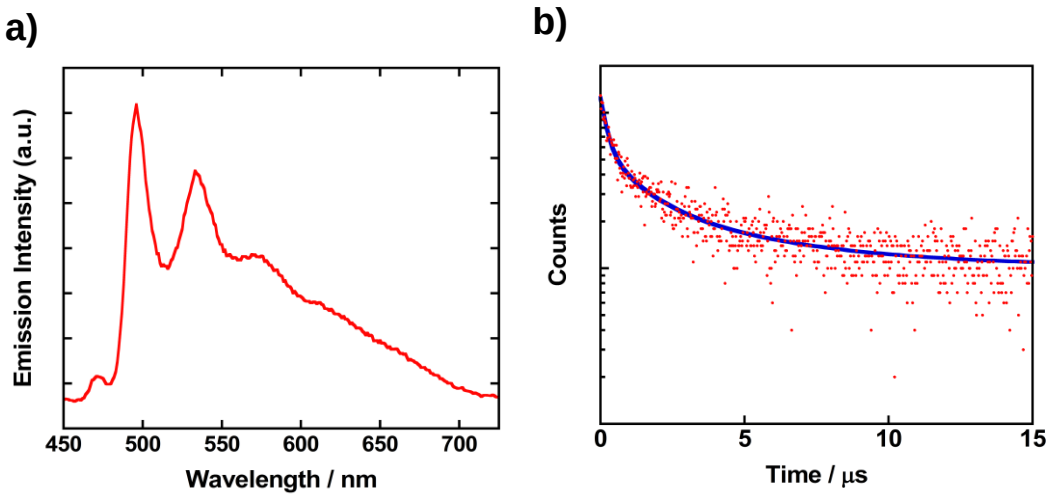

Fig. S3 a) An emission spectrum of **[PtCl$_2$(bpyMV2)]$^{4+}$** in MED glass at 77 K (excitation at 380 nm), where MED is a 4/4/1 (v/v/v) methanol/ethanol/DMF mixture. b) An emission decay profile of **[PtCl$_2$(bpyMV2)]$^{4+}$** in MED glass at 77 K. The emission was monitored at 500 nm. The blue line shows a calculated one according to a triple exponential function.

Table S1. Emission wavelengths and lifetimes for **[PtCl$_2$(bpyMV2)]$^{4+}$** in MED glass at 77 K.

λ_{em} / nm	Lifetimes[a]	Relative contribution	$\langle\tau\rangle$[b] / μs
496, 533,	τ_1 = 1.24 μs	χ_1 = 26.6 %	
575, 612	τ_2 = 4.56 μs	χ_2 = 15.8 %	3.14 μs
	τ_3 = 0.234 μs	χ_3 = 57.6 %	

[a]Lifetimes were estimated by fitting the decay at 500 nm to a triple exponential function. [b]Average lifetime $\langle\tau\rangle$ was estimated using a definition of $\langle\tau\rangle = \Sigma\, a_i\tau_i^2 / \Sigma\, a_i\tau_i$, where a_i is the relative contribution of the corresponding lifetime τ_i.[S19]

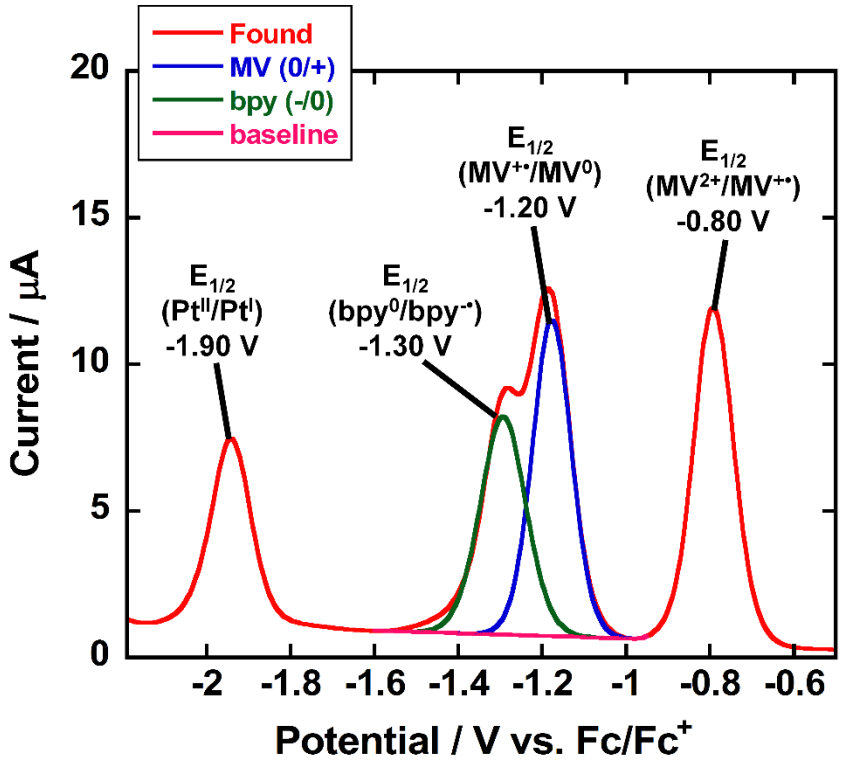

Fig. S4 A square wave voltammogram of **[PtCl$_2$(bpyMV2)]$^{4+}$** (1 mM) in a DMF solution containing 0.1 M TBAP at room temperature under Ar atmosphere. For each case, deconvolution was carried out for the potential range where the reduction peaks of viologen and bpy are overlapped (−0.95 ~ −1.6 V vs. Fc/Fc$^+$).

(a)

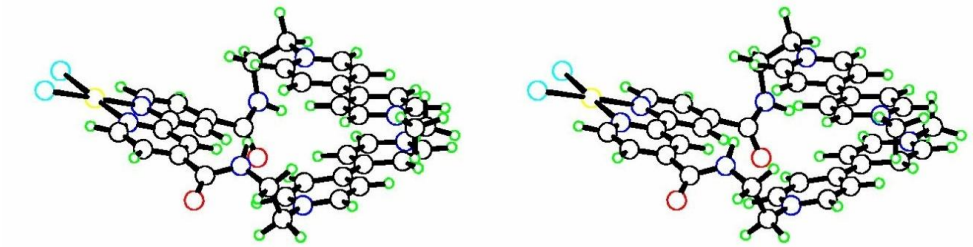

(b)

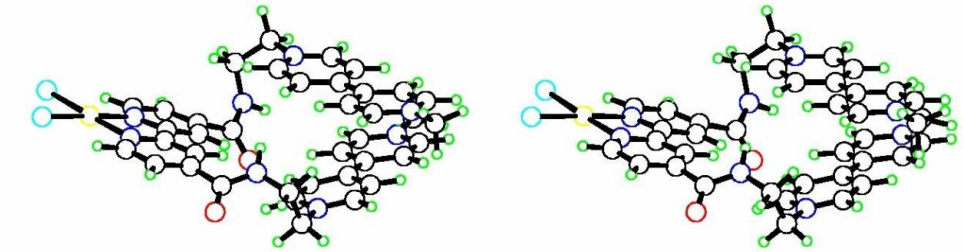

Fig. S5 Stereo views showing the geometries for (a) the closed-shell singlet state and (b) the open-shell singlet state of the two-electron-reduced form of **[PtCl$_2$(bpyMV2)]$^{4+}$**. The structures were optimized at the M06 and UM06 level of DFT calculations with the effect of water solvation taken into consideration using the polarizable continuum model (PCM) method, where the SDD basis set was used for Pt and the 6-31G** basis set for H, C, N, O, and Cl.

Table S2. Geometry optimized by DFT for the closed-shell singlet state of the two-electron-reduced form of **$[PtCl_2(bpyMV2)]^{4+}$**, i.e., **$[PtCl_2(bpy)\text{-}(MV^+)_2]^{2+}$**. Optimized at the M06/SDD(Pt)/6-31G**(HCNOCl) level using PCM.[a]

Atom	X	Y	Z
Pt1	-5.249545	0.228408	0.201542
N2	-3.542235	1.261716	-0.293436
C3	-1.102116	2.417406	-0.916936
C4	-2.436754	0.484640	-0.426765
C5	-3.450680	2.584815	-0.482337
C6	-2.246031	3.200367	-0.788690
C7	-1.211133	1.042046	-0.755438
H8	-4.376560	3.142772	-0.373572
H9	-2.218195	4.276226	-0.934150
H10	-0.326874	0.425648	-0.887134
N11	-3.926446	-1.330054	0.006783
C12	-1.941355	-3.241449	-0.276308
C13	-4.225969	-2.635580	0.095807
C14	-2.649084	-0.949614	-0.241214
C15	-1.635468	-1.888552	-0.350821
C16	-3.264355	-3.618227	-0.070665
H17	-5.268965	-2.865971	0.295146
H18	-0.615794	-1.562670	-0.532307
H19	-3.540451	-4.667227	-0.038607
Cl20	-6.620087	2.138628	0.361161
Cl21	-7.086147	-1.125046	0.793697
C22	0.236004	2.966253	-1.322535
C23	-0.903180	-4.285572	-0.552521
O24	0.869947	2.405067	-2.210544
O25	-1.191904	-5.301681	-1.168229
N26	0.663082	4.090645	-0.698170
H27	1.528015	4.461066	-1.080117
N28	0.354217	-3.987409	-0.135296
H29	0.499149	-3.230096	0.518255
C30	0.290095	4.536328	0.633196

H31	-0.550313	3.933429	0.986874
H32	-0.062407	5.573726	0.615503
C33	1.454263	4.456920	1.611828
H34	2.186595	5.238698	1.388581
H35	1.080424	4.639161	2.626532
C36	1.472917	-4.828348	-0.508183
H37	2.221536	-4.806834	0.290486
H38	1.115346	-5.857978	-0.609781
C39	2.085042	-4.387699	-1.832360
H40	2.818028	-5.122962	-2.177313
H41	1.305843	-4.309504	-2.598035
N42	2.175749	3.180532	1.566808
C43	3.609028	0.736601	1.615592
C44	1.517038	1.978976	1.525085
C45	3.539461	3.170105	1.598949
C46	4.250036	2.008042	1.644175
C47	2.181803	0.790818	1.523477
H48	0.432251	2.025607	1.523173
H49	4.026502	4.140683	1.616210
H50	5.330088	2.098665	1.697041
H51	1.576840	-0.110832	1.489154
C52	4.336968	-0.482606	1.737513
N53	5.778807	-2.888551	2.087604
C54	3.703820	-1.757466	1.774662
C55	5.759439	-0.514822	1.884854
C56	6.430812	-1.690676	2.037298
C57	4.423399	-2.904663	1.939361
H58	2.627428	-1.860553	1.680976
H59	6.351951	0.393185	1.894777
H60	7.509823	-1.731768	2.145981
H61	3.955154	-3.883320	1.986920
N62	2.760640	-3.091438	-1.725625
C63	4.068626	-0.608168	-1.394519
C64	2.087709	-1.915480	-1.922491
C65	4.069232	-3.040184	-1.345914
C66	4.728783	-1.854509	-1.209001

C67	2.688622	-0.702082	-1.755967
H68	1.064384	-2.010709	-2.273831
H69	4.561892	-3.997361	-1.194368
H70	5.779681	-1.905171	-0.945873
H71	2.090626	0.182983	-1.964795
C72	4.766024	0.637070	-1.298242
N73	6.167775	3.081714	-1.177018
C74	4.125230	1.890539	-1.497575
C75	6.168030	0.705820	-1.035342
C76	6.818968	1.902344	-0.970919
C77	4.827537	3.059708	-1.422025
H78	3.062278	1.967854	-1.717944
H79	6.767729	-0.186173	-0.894031
H80	7.883409	1.973125	-0.771503
H81	4.360875	4.028996	-1.571073
C82	6.854366	4.359222	-1.010633
H83	6.676780	4.754878	-0.004773
H84	6.483276	5.071443	-1.750398
H85	7.925598	4.217797	-1.159795
C86	6.515760	-4.145738	2.166768
H87	7.496359	-3.964950	2.609210
H88	6.641530	-4.575275	1.166982
H89	5.967889	-4.849958	2.796414

---

[a]Part of the Gaussian output file:

SCF Done: E(RM06) = -3097.51161660 A.U. after 6 cycles

	1	2	3
	A	A	A
Frequencies --	23.3941	35.1806	41.5035
Red. masses --	7.6593	5.8555	7.0154

Zero-point correction= 0.717285 (Hartree/Particle)

Thermal correction to Energy= 0.762366

Thermal correction to Enthalpy= 0.763310

Thermal correction to Gibbs Free Energy= 0.641062

Sum of electronic and zero-point Energies= -3096.794332

Sum of electronic and thermal Energies= -3096.749250

Sum of electronic and thermal Enthalpies= -3096.748306

Sum of electronic and thermal Free Energies= -3096.870554

Item	Value	Threshold	Converged?
Maximum Force	0.000414	0.000450	YES
RMS Force	0.000056	0.000300	YES

Table S3. Geometry optimized by DFT for the open-shell singlet state of the two-electron-reduced form of **$[PtCl_2(bpyMV2)]^{4+}$**, i.e., **$[PtCl_2(bpy)\text{-}(MV^+)_2]^{2+}$**. Optimized at the UM06/SDD(Pt)/6-31G**(HCNOCl) level of broken symmetry approach using PCM.[a]

Atom	X	Y	Z	Spin Density
Pt1	-5.272313	0.227367	0.189126	0.000000
N2	-3.547715	1.269015	-0.219298	0.000003
C3	-1.106439	2.426963	-0.833064	-0.000004
C4	-2.442930	0.491751	-0.356777	-0.000004
C5	-3.452869	2.594521	-0.389175	-0.000003
C6	-2.247281	3.211467	-0.689031	0.000004
C7	-1.217036	1.050732	-0.680656	0.000004
H8	-4.378712	3.152063	-0.277798	0.000000
H9	-2.218136	4.288612	-0.824473	0.000000
H10	-0.334337	0.434955	-0.824071	0.000000
N11	-3.940610	-1.327754	0.025013	-0.000002
C12	-1.945760	-3.234947	-0.225394	0.000002
C13	-4.238948	-2.634201	0.103299	0.000002
C14	-2.657830	-0.944269	-0.189357	0.000002
C15	-1.640356	-1.881094	-0.283592	-0.000003
C16	-3.272037	-3.614117	-0.046626	-0.000003
H17	-5.285600	-2.868242	0.277389	0.000000
H18	-0.617776	-1.551111	-0.440918	0.000000
H19	-3.547119	-4.663634	-0.025100	0.000000
Cl20	-6.642581	2.140434	0.340110	0.000000
Cl21	-7.144680	-1.139864	0.625737	0.000000
C22	0.225783	2.973078	-1.260827	0.000001
C23	-0.905757	-4.279190	-0.495078	0.000000
O24	0.843896	2.407168	-2.156926	0.000000
O25	-1.193891	-5.296027	-1.110154	0.000000
N26	0.661841	4.102507	-0.652083	0.000000
H27	1.518044	4.473422	-1.052750	0.000000
N28	0.351950	-3.983078	-0.077322	0.000000
H29	0.500676	-3.226370	0.576190	0.000000
C30	0.321745	4.543045	0.689953	0.000000

H31	-0.507666	3.936793	1.063583	0.000000
H32	-0.033813	5.579502	0.684521	0.000000
C33	1.512039	4.464614	1.636029	0.000000
H34	2.239089	5.244001	1.388103	0.000000
H35	1.167485	4.651869	2.660176	0.000000
C36	1.467558	-4.827531	-0.452601	0.000000
H37	2.224027	-4.796405	0.338146	0.000000
H38	1.110363	-5.858659	-0.539400	0.000000
C39	2.066927	-4.401672	-1.787596	0.000000
H40	2.795740	-5.141624	-2.131127	0.000000
H41	1.281058	-4.331063	-2.547100	0.000000
N42	2.230017	3.186449	1.575761	0.000000
C43	3.661551	0.740585	1.603094	0.000001
C44	1.570201	1.985351	1.536158	0.000001
C45	3.594073	3.174466	1.591974	0.000001
C46	4.304052	2.011584	1.625239	-0.000002
C47	2.233346	0.796318	1.526252	-0.000001
H48	0.485642	2.032448	1.543989	0.000000
H49	4.082217	4.144649	1.604987	0.000000
H50	5.384861	2.100715	1.663672	0.000000
H51	1.626113	-0.104222	1.495797	0.000000
C52	4.389956	-0.479005	1.714974	0.000001
N53	5.833368	-2.886303	2.047980	0.000000
C54	3.755279	-1.752513	1.767740	-0.000002
C55	5.814962	-0.513263	1.835689	-0.000001
C56	6.486621	-1.689819	1.980612	0.000001
C57	4.475491	-2.900403	1.924087	0.000002
H58	2.677047	-1.852742	1.693502	0.000000
H59	6.409493	0.393502	1.830018	0.000000
H60	7.567383	-1.732675	2.069284	0.000000
H61	4.006450	-3.878034	1.983455	0.000000
N62	2.744966	-3.105238	-1.701881	0.000000
C63	4.055381	-0.619222	-1.404802	0.000001
C64	2.067289	-1.931140	-1.892042	0.000001
C65	4.060560	-3.050901	-1.347959	0.000001
C66	4.721162	-1.863706	-1.229047	-0.000001

C67	2.669197	-0.716310	-1.739931	-0.000001
H68	1.038599	-2.027852	-2.226468	0.000000
H69	4.557375	-4.006760	-1.201788	0.000000
H70	5.776762	-1.911715	-0.985046	0.000000
H71	2.067226	0.167259	-1.942992	0.000000
C72	4.751582	0.628070	-1.325397	0.000000
N73	6.149014	3.075979	-1.249109	0.000000
C74	4.100240	1.879471	-1.500203	-0.000001
C75	6.160570	0.700274	-1.104861	0.000000
C76	6.809769	1.898727	-1.062522	0.000000
C77	4.801081	3.050686	-1.447296	0.000001
H78	3.028307	1.952689	-1.673399	0.000000
H79	6.766772	-0.190014	-0.981621	0.000000
H80	7.879826	1.972849	-0.897703	0.000000
H81	4.326828	4.019165	-1.576965	0.000000
C82	6.837994	4.355171	-1.108229	0.000000
H83	6.688599	4.754820	-0.099347	0.000000
H84	6.445318	5.063642	-1.840474	0.000000
H85	7.904747	4.214322	-1.287194	0.000000
C86	6.569937	-4.144245	2.117913	0.000000
H87	7.556796	-3.964178	2.546573	0.000000
H88	6.681443	-4.575008	1.116973	0.000000
H89	6.030261	-4.847405	2.755702	0.000000

---

[a]Part of the Gaussian output file:

SCF Done: E(UM06) = -3097.51162153 A.U. after 29 cycles

Annihilation of the first spin contaminant:

S**2 before annihilation 0.0000, after 0.0000

	1	2	3
	A	A	A
Frequencies --	18.4220	34.2255	36.9745
Red. masses --	7.6063	5.8037	6.6053

Zero-point correction= 0.716808 (Hartree/Particle)

Thermal correction to Energy=	0.762144
Thermal correction to Enthalpy=	0.763088
Thermal correction to Gibbs Free Energy=	0.639537
Sum of electronic and zero-point Energies=	-3096.794814
Sum of electronic and thermal Energies=	-3096.749477
Sum of electronic and thermal Enthalpies=	-3096.748533
Sum of electronic and thermal Free Energies=	-3096.872084

Item	Value	Threshold	Converged?
Maximum Force	0.000096	0.000450	YES
RMS Force	0.000014	0.000300	YES

Table S4. Electronic transitions computed by TD-DFT for the closed-shell singlet state of **$[PtCl_2(bpy)\text{-}(MV^+)_2]^{2+}$**, for which part of the Gaussian output is shown. Relevant MO's are shown below:

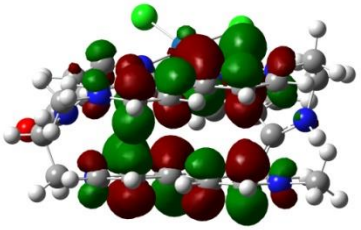

MO203 (LUMO+8)

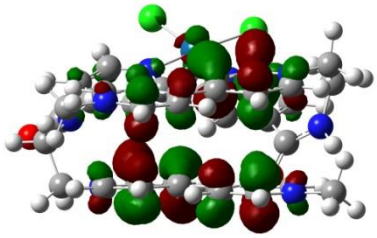

MO202(LUMO+7)

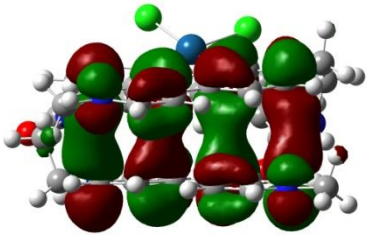

MO200 (LUMO+5)

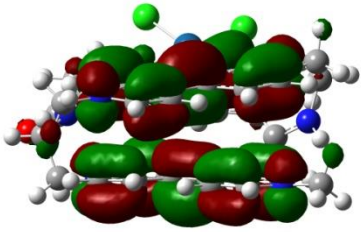

MO196 (LUMO+1)

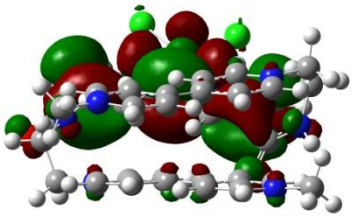

MO195 (LUMO)

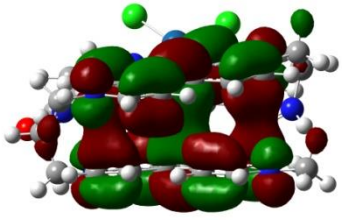

MO194 (HOMO)

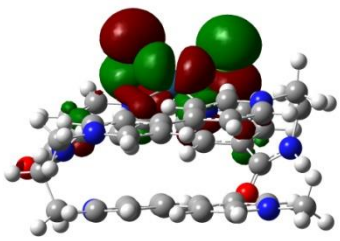

MO193 (HOMO-1)

Excitation energies and oscillator strengths (λ > 210 nm, f > 0.02 only):

Excited State 2:	Singlet-A	1.4502 eV	854.92 nm	f=0.1872	<S**2>=0.000
194 ->195	0.13260				
194 ->196	0.72995				
194 <-196	-0.22548				
Excited State 7:	Singlet-A	2.4345 eV	509.27 nm	f=0.0812	<S**2>=0.000
194 ->200	0.56687				
194 ->202	0.25317				
194 ->203	-0.31311				
Excited State 10:	Singlet-A	2.8913 eV	428.82 nm	f=0.2370	<S**2>=0.000
189 ->196	0.15735				
193 ->195	0.24646				
194 ->200	0.35302				
194 ->202	-0.33652				
194 ->203	0.38995				
Excited State 14:	Singlet-A	3.1946 eV	388.10 nm	f=0.0470	<S**2>=0.000
192 ->195	0.27404				
192 ->199	-0.23522				
194 ->205	0.16930				
194 ->206	0.14194				
194 ->207	0.53957				
Excited State 15:	Singlet-A	3.1976 eV	387.75 nm	f=0.0427	<S**2>=0.000
192 ->195	0.39556				
192 ->198	0.12800				
192 ->199	-0.37003				
194 ->206	-0.10244				
194 ->207	-0.36886				
Excited State 17:	Singlet-A	3.2522 eV	381.24 nm	f=0.0991	<S**2>=0.000
190 ->199	0.21045				
192 ->195	0.44169				
192 ->198	-0.10408				
192 ->199	0.44818				
Excited State 20:	Singlet-A	3.3043 eV	375.23 nm	f=0.1525	<S**2>=0.000
192 ->195	-0.10441				
194 ->201	0.11715				
194 ->202	0.10759				
194 ->205	0.62780				
194 ->207	-0.16714				
Excited State 25:	Singlet-A	3.9412 eV	314.59 nm	f=0.0302	<S**2>=0.000
185 ->195	0.11139				
186 ->195	0.19199				
187 ->195	0.39525				
188 ->195	0.21718				
189 ->196	0.33561				

192 ->197 0.12963
193 ->198 0.24315

Excited State 26: Singlet-A 3.9546 eV 313.52 nm f=0.0637 <S**2>=0.000
188 ->195 0.60891
188 ->196 -0.12150
189 ->196 -0.25207
190 ->196 0.11914

Excited State 27: Singlet-A 3.9736 eV 312.02 nm f=0.4776 <S**2>=0.000
186 ->195 -0.13235
187 ->195 -0.22591
188 ->195 0.17568
189 ->195 0.15132
189 ->196 0.48473
192 ->197 -0.16174
193 ->198 -0.22791
194 ->200 -0.11578

Excited State 29: Singlet-A 4.0494 eV 306.18 nm f=0.0601 <S**2>=0.000
187 ->195 -0.11836
192 ->197 -0.35889
193 ->197 0.50389
193 ->198 0.20574
193 ->199 0.13360

Excited State 30: Singlet-A 4.0965 eV 302.66 nm f=0.0480 <S**2>=0.000
189 ->195 0.19166
191 ->197 -0.32121
192 ->197 0.28757
192 ->198 -0.13613
193 ->197 0.33331
193 ->198 -0.31736

Excited State 31: Singlet-A 4.1072 eV 301.87 nm f=0.0264 <S**2>=0.000
183 ->195 -0.13460
189 ->195 0.58461
189 ->196 -0.13342
192 ->197 -0.13296
193 ->197 -0.11032
193 ->198 0.20900

Excited State 36: Singlet-A 4.1796 eV 296.64 nm f=0.1873 <S**2>=0.000
185 ->196 -0.25707
186 ->195 0.14450
186 ->196 0.54293
187 ->196 -0.22079
194 ->209 0.14285

Excited State 37: Singlet-A 4.2056 eV 294.81 nm f=0.1564 <S**2>=0.000
181 ->195 0.17382
182 ->195 -0.16219
184 ->195 0.43959
184 ->197 -0.11246

187 ->195 -0.22495
192 ->197 0.19270
193 ->198 0.22864

Excited State 38: Singlet-A 4.2359 eV 292.70 nm f=0.1022 <S**2>=0.000
182 ->196 0.11883
185 ->195 0.15382
185 ->196 0.53940
187 ->195 -0.10857
187 ->196 -0.33732

Excited State 40: Singlet-A 4.2568 eV 291.26 nm f=0.0225 <S**2>=0.000
183 ->195 -0.16639
191 ->198 0.21499
192 ->198 0.56101
192 ->199 0.16712
193 ->197 0.14992

Excited State 41: Singlet-A 4.3157 eV 287.29 nm f=0.2479 <S**2>=0.000
181 ->195 0.13261
183 ->195 0.10941
184 ->195 0.34748
185 ->195 -0.12275
186 ->195 -0.15338
187 ->195 0.37315
187 ->196 -0.11302
192 ->197 -0.23052
192 ->198 0.10932
193 ->198 -0.17625

Excited State 43: Singlet-A 4.3381 eV 285.80 nm f=0.0228 <S**2>=0.000
185 ->195 -0.19773
186 ->195 -0.19731
190 ->197 0.59230

Excited State 44: Singlet-A 4.3454 eV 285.32 nm f=0.2207 <S**2>=0.000
183 ->195 0.14940
184 ->195 0.11182
185 ->195 0.33909
186 ->195 0.33139
190 ->197 0.32244
192 ->197 -0.20296
192 ->198 0.11105
193 ->198 -0.17303

Excited State 53: Singlet-A 4.5689 eV 271.37 nm f=0.0204 <S**2>=0.000
180 ->196 -0.22806
182 ->195 0.12242
182 ->196 0.54285
183 ->196 -0.13978
184 ->196 -0.10979
185 ->196 -0.14179
186 ->196 -0.12017
188 ->196 0.19163

Excited State 71:	Singlet-A	5.1208 eV	242.12 nm	f=0.0273	<S**2>=0.000
182 ->198	-0.10203				
184 ->198	-0.10748				
186 ->197	-0.10896				
187 ->198	-0.28767				
189 ->198	0.54854				
189 ->199	0.10717				
Excited State 73:	Singlet-A	5.1443 eV	241.01 nm	f=0.0449	<S**2>=0.000
171 ->195	0.11634				
175 ->195	0.10039				
176 ->195	-0.10811				
177 ->199	-0.16046				
183 ->197	-0.12701				
183 ->198	0.25207				
184 ->197	0.13654				
185 ->198	0.17003				
186 ->198	0.22471				
187 ->198	0.28791				
187 ->199	0.10989				
189 ->198	0.25693				
Excited State 79:	Singlet-A	5.2095 eV	238.00 nm	f=0.0520	<S**2>=0.000
175 ->195	-0.11632				
176 ->195	0.51695				
176 ->196	-0.10518				
178 ->195	-0.13269				
187 ->197	-0.13295				
193 ->200	-0.28662				
Excited State 81:	Singlet-A	5.2547 eV	235.95 nm	f=0.0264	<S**2>=0.000
175 ->195	0.61121				
175 ->196	-0.12671				
176 ->195	0.13361				
187 ->198	-0.11328				
Excited State 100:	Singlet-A	5.4936 eV	225.69 nm	f=0.0233	<S**2>=0.000
176 ->198	-0.10559				
176 ->199	0.35573				
184 ->197	-0.19889				
184 ->198	0.27638				
184 ->199	0.12284				
185 ->198	0.12195				
190 ->202	-0.28469				
190 ->203	-0.20308				
191 ->202	-0.10727				
Excited State 122:	Singlet-A	5.7474 eV	215.72 nm	f=0.0262	<S**2>=0.000
170 ->195	0.17534				
171 ->195	-0.17895				
183 ->199	-0.22606				
184 ->199	-0.12980				
185 ->199	0.44845				

186 ->199	-0.30688				
Excited State 123:	Singlet-A	5.7557 eV	215.41 nm	f=0.0323	<S**2>=0.000
169 ->195	-0.11551				
170 ->195	0.50766				
170 ->196	-0.10625				
171 ->195	-0.17786				
177 ->197	0.13263				
183 ->199	0.20068				
185 ->199	-0.15670				
193 ->204	0.16807				
Excited State 127:	Singlet-A	5.8140 eV	213.25 nm	f=0.0502	<S**2>=0.000
169 ->195	-0.11762				
170 ->195	0.27072				
171 ->195	0.35159				
174 ->195	-0.11681				
177 ->197	-0.22213				
181 ->197	0.14709				
181 ->198	-0.18132				
183 ->199	-0.14439				
192 ->203	-0.12740				
Excited State 128:	Singlet-A	5.8304 eV	212.65 nm	f=0.0267	<S**2>=0.000
177 ->197	0.10133				
185 ->201	-0.10137				
186 ->201	0.29988				
187 ->201	-0.15365				
189 ->202	0.22556				
189 ->203	-0.27059				
192 ->202	0.12745				
192 ->203	-0.17889				
192 ->206	-0.14323				
194 ->220	0.11467				
194 ->222	-0.14318				
Excited State 129:	Singlet-A	5.8325 eV	212.58 nm	f=0.0646	<S**2>=0.000
169 ->195	0.13767				
177 ->197	0.29226				
181 ->197	-0.11582				
181 ->198	0.11556				
186 ->201	-0.15764				
189 ->202	-0.12256				
189 ->203	0.14726				
192 ->202	0.20115				
192 ->203	-0.27739				
192 ->206	-0.22415				
193 ->208	0.13232				
Excited State 132:	Singlet-A	5.8491 eV	211.97 nm	f=0.0516	<S**2>=0.000
169 ->195	0.17319				
171 ->195	0.16331				
174 ->195	-0.10835				
177 ->197	0.29027				

179 ->197	0.18366
180 ->197	0.29529
192 ->202	-0.12612
192 ->203	0.17836
192 ->206	0.17316
193 ->208	-0.21806

Table S5. Electronic transitions computed by TD-DFT for the open-shell singlet state of **$[PtCl_2(bpy)\text{-}(MV^+)_2]^{2+}$**, for which part of the Gaussian output is shown.

Relevant MO's (only α orbitals) are shown below:

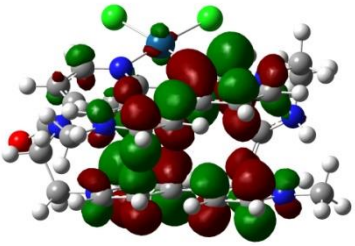

MO203α (LUMO+8)

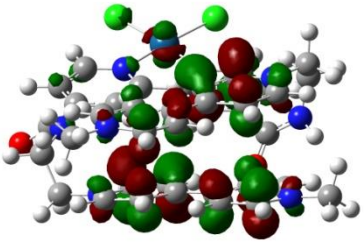

MO202α(LUMO+7)

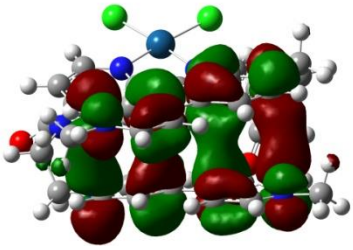

MO200α (LUMO+5)

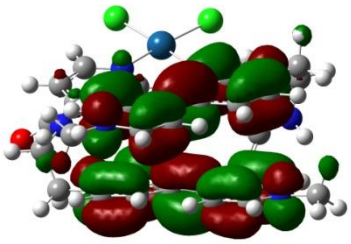

MO196α (LUMO+1)

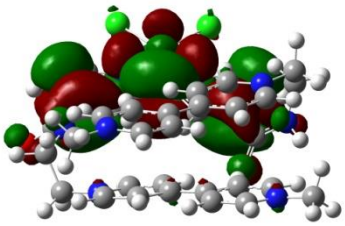

MO195α (LUMO)

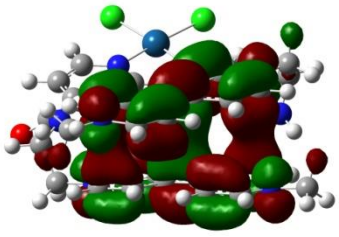

MO194α (HOMO)

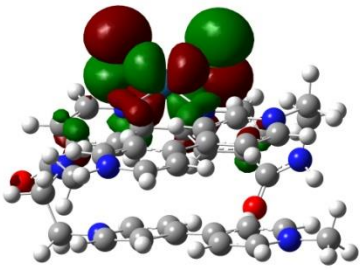

MO193α (HOMO-1)

Excitation energies and oscillator strengths (λ > 210 nm, f > 0.02 only):

Excited State 4:	1.000-A	1.4570 eV	850.94 nm	f=0.1882	<S**2>=0.000
194A ->195A	0.10123				
194A ->196A	0.73438				
194B ->195B	0.10123				
194B ->196B	0.73438				
194A <-196A	-0.22590				
194B <-196B	-0.22590				
Excited State 16:	1.000-A	2.4340 eV	509.38 nm	f=0.0832	<S**2>=0.000
194A ->200A	0.56867				
194A ->202A	0.23914				
194A ->203A	-0.31837				
194B ->200B	0.56867				
194B ->202B	0.23914				
194B ->203B	-0.31836				
Excited State 26:	1.000-A	2.8942 eV	428.40 nm	f=0.2422	<S**2>=0.000
189A ->196A	0.16276				
193A ->195A	0.20679				
194A ->200A	0.35625				
194A ->202A	-0.33168				
194A ->203A	0.41449				
189B ->196B	0.16276				
193B ->195B	0.20679				
194B ->200B	0.35625				
194B ->202B	-0.33168				
194B ->203B	0.41449				
Excited State 34:	1.000-A	3.1891 eV	388.78 nm	f=0.0749	<S**2>=0.000
192A ->195A	0.46399				
192A ->198A	0.19114				
192A ->199A	-0.45986				
192B ->195B	0.46399				
192B ->198B	0.19113				
192B ->199B	-0.45986				
Excited State 38:	1.000-A	3.2590 eV	380.43 nm	f=0.1149	<S**2>=0.000
190A ->199A	0.10266				
192A ->195A	0.47571				
192A ->198A	-0.13260				
192A ->199A	0.44705				
194A ->205A	0.10474				
190B ->199B	0.10266				
192B ->195B	0.47571				
192B ->198B	-0.13260				
192B ->199B	0.44705				
194B ->205B	0.10474				
Excited State 42:	1.000-A	3.3099 eV	374.58 nm	f=0.1555	<S**2>=0.000
194A ->201A	0.11732				
194A ->202A	0.12050				

194A ->205A 0.62929
194A ->207A -0.17246
194B ->201B 0.11732
194B ->202B 0.12050
194B ->205B 0.62929
194B ->207B -0.17246

Excited State 57: 1.000-A 3.9398 eV 314.70 nm f=0.0427 <S**2>=0.000
185A ->195A 0.12225
186A ->195A 0.17620
187A ->195A 0.43183
189A ->196A 0.37682
192A ->197A 0.12765
193A ->198A 0.23525
185B ->195B 0.12225
186B ->195B 0.17620
187B ->195B 0.43183
189B ->196B 0.37682
192B ->197B 0.12765
193B ->198B 0.23525

Excited State 61: 1.000-A 3.9713 eV 312.20 nm f=0.5187 <S**2>=0.000
186A ->195A -0.11337
187A ->195A -0.22005
188A ->195A 0.12769
189A ->195A 0.13083
189A ->196A 0.51905
192A ->197A -0.17479
193A ->198A -0.21082
194A ->200A -0.12189
186B ->195B -0.11337
187B ->195B -0.22005
188B ->195B 0.12768
189B ->195B 0.13083
189B ->196B 0.51905
192B ->197B -0.17479
193B ->198B -0.21082
194B ->200B -0.12189

Excited State 66: 1.000-A 4.0491 eV 306.20 nm f=0.0604 <S**2>=0.000
187A ->195A -0.10239
192A ->197A -0.36473
193A ->197A 0.50210
193A ->198A 0.24066
187B ->195B -0.10239
192B ->197B -0.36473
193B ->197B 0.50209
193B ->198B 0.24067

Excited State 70: 1.000-A 4.1022 eV 302.24 nm f=0.0780 <S**2>=0.000
189A ->195A 0.29452
192A ->197A -0.30587
192A ->198A 0.10104
193A ->197A -0.34928

193A ->198A 0.35788
193A ->199A 0.12768
189B ->195B 0.29451
192B ->197B -0.30587
192B ->198B 0.10104
193B ->197B -0.34928
193B ->198B 0.35788
193B ->199B 0.12768

Excited State 81: 1.000-A 4.1827 eV 296.42 nm f=0.1763 <S**2>=0.000
185A ->196A -0.25170
186A ->195A 0.11907
186A ->196A 0.56520
187A ->196A -0.18336
194A ->209A 0.13646
185B ->196B -0.25170
186B ->195B 0.11907
186B ->196B 0.56521
187B ->196B -0.18336
194B ->209B 0.13645

Excited State 82: 1.000-A 4.2030 eV 294.99 nm f=0.1613 <S**2>=0.000
181A ->195A 0.16866
182A ->195A -0.15878
184A ->195A 0.43280
184A ->197A -0.11176
187A ->195A -0.23141
192A ->197A 0.18850
193A ->198A 0.23557
181B ->195B 0.16864
182B ->195B -0.15879
184B ->195B 0.43281
184B ->197B -0.11177
187B ->195B -0.23140
192B ->197B 0.18847
193B ->198B 0.23560

Excited State 86: 1.000-A 4.2392 eV 292.47 nm f=0.1136 <S**2>=0.000
182A ->196A 0.12078
185A ->195A 0.12587
185A ->196A 0.54163
186A ->196A 0.10774
187A ->196A -0.34258
182B ->196B 0.12078
185B ->195B 0.12587
185B ->196B 0.54163
186B ->196B 0.10774
187B ->196B -0.34258

Excited State 92: 1.000-A 4.3136 eV 287.43 nm f=0.2432 <S**2>=0.000
181A ->195A 0.13371
183A ->195A 0.10541
184A ->195A 0.35673
185A ->195A -0.13865

186A ->195A -0.18171
187A ->195A 0.36730
192A ->197A -0.22852
193A ->198A -0.17665
181B ->195B 0.13373
183B ->195B 0.10541
184B ->195B 0.35673
185B ->195B -0.13866
186B ->195B -0.18171
187B ->195B 0.36730
192B ->197B -0.22853
193B ->198B -0.17665

Excited State 98: 1.000-A 4.3439 eV 285.42 nm f=0.2447 <S**2>=0.000
183A ->195A 0.16575
184A ->195A 0.11306
185A ->195A 0.40574
186A ->195A 0.36537
190A ->197A 0.11518
192A ->197A -0.21713
192A ->198A 0.10888
193A ->198A -0.18509
183B ->195B 0.16575
184B ->195B 0.11306
185B ->195B 0.40574
186B ->195B 0.36537
190B ->197B 0.11518
192B ->197B -0.21713
192B ->198B 0.10888
193B ->198B -0.18509

Excited State 151: 1.000-A 5.0139 eV 247.28 nm f=0.0221 <S**2>=0.000
176A ->195A 0.12587
177A ->195A 0.10666
183A ->197A 0.23762
183A ->198A -0.21955
187A ->197A 0.27209
187A ->199A 0.11522
188A ->197A 0.14348
188A ->198A 0.11823
189A ->197A 0.35057
189A ->198A 0.13195
176B ->195B 0.12587
177B ->195B 0.10668
183B ->197B 0.23762
183B ->198B -0.21956
187B ->197B 0.27209
187B ->199B 0.11522
188B ->197B 0.14347
188B ->198B 0.11823
189B ->197B 0.35066
189B ->198B 0.13198

Excited State 156: 1.000-A 5.1131 eV 242.48 nm f=0.0226 <S**2>=0.000

186A ->197A -0.10800
187A ->198A -0.25571
187A ->199A -0.10053
189A ->198A 0.55504
189A ->199A 0.13823
186B ->197B -0.10800
187B ->198B -0.25571
187B ->199B -0.10053
189B ->198B 0.55503
189B ->199B 0.13822

Excited State 160: 1.000-A 5.1409 eV 241.17 nm f=0.0416 <S**2>=0.000
171A ->195A 0.11191
176A ->195A -0.10437
177A ->199A -0.23483
183A ->197A -0.14426
183A ->198A 0.24146
184A ->197A 0.12328
185A ->198A 0.14987
186A ->198A 0.17448
187A ->198A 0.29508
187A ->199A 0.10841
189A ->198A 0.23177
171B ->195B 0.11191
176B ->195B -0.10437
177B ->199B -0.23483
183B ->197B -0.14426
183B ->198B 0.24146
184B ->197B 0.12329
185B ->198B 0.14987
186B ->198B 0.17447
187B ->198B 0.29508
187B ->199B 0.10841
189B ->198B 0.23174

Excited State 171: 1.000-A 5.1990 eV 238.48 nm f=0.0458 <S**2>=0.000
176A ->195A 0.49232
178A ->195A -0.16545
187A ->197A -0.11876
193A ->200A 0.36966
176B ->195B 0.49231
178B ->195B -0.16546
187B ->197B -0.11876
193B ->200B 0.36959

Excited State 173: 1.000-A 5.2064 eV 238.14 nm f=0.0213 <S**2>=0.000
176A ->195A -0.30573
187A ->197A 0.13148
193A ->200A 0.57916
176B ->195B -0.30572
187B ->197B 0.13148
193B ->200B 0.57930

Excited State 174: 1.000-A 5.2231 eV 237.38 nm f=0.0224 <S**2>=0.000

182A ->198A 0.17612
184A ->198A 0.13136
185A ->197A 0.31536
185A ->198A -0.20467
186A ->197A 0.25815
186A ->198A -0.18244
187A ->197A -0.21033
187A ->198A 0.14409
189A ->198A 0.24539
182B ->198B 0.17612
184B ->198B 0.13136
185B ->197B 0.31537
185B ->198B -0.20467
186B ->197B 0.25816
186B ->198B -0.18244
187B ->197B -0.21033
187B ->198B 0.14409
189B ->198B 0.24539

Excited State 215: 1.000-A 5.4947 eV 225.64 nm f=0.0347 <S**2>=0.000
176A ->199A -0.12304
184A ->198A -0.10709
190A ->202A 0.42757
190A ->203A 0.28499
191A ->202A 0.33816
191A ->203A 0.21486
176B ->199B -0.12304
184B ->198B -0.10709
190B ->202B 0.42757
190B ->203B 0.28499
191B ->202B 0.33815
191B ->203B 0.21486

Excited State 255: 1.000-A 5.7077 eV 217.22 nm f=0.0219 <S**2>=0.000
171A ->195A 0.12321
183A ->198A -0.14586
183A ->199A 0.50709
184A ->199A -0.12237
185A ->199A 0.22688
186A ->199A -0.28658
171B ->195B 0.12321
183B ->198B -0.14586
183B ->199B 0.50709
184B ->199B -0.12237
185B ->199B 0.22688
186B ->199B -0.28658

Excited State 263: 1.000-A 5.7488 eV 215.67 nm f=0.0254 <S**2>=0.000
169A ->195A -0.11964
170A ->195A 0.61061
170A ->196A -0.10015
177A ->197A 0.10168
183A ->199A 0.10702
169B ->195B -0.11963

170B ->195B	0.61059				
170B ->196B	-0.10015				
177B ->197B	0.10167				
183B ->199B	0.10703				

Excited State 269:	1.000-A	5.8005 eV	213.75 nm	f=0.0439	<S**2>=0.000
169A ->195A	-0.10289				
170A ->195A	0.12550				
171A ->195A	0.40948				
174A ->195A	-0.13589				
174A ->196A	0.10925				
177A ->197A	-0.22936				
181A ->198A	0.19696				
183A ->199A	-0.16531				
186A ->200A	-0.12016				
187A ->198A	-0.11608				
169B ->195B	-0.10289				
170B ->195B	0.12550				
171B ->195B	0.40948				
174B ->195B	-0.13589				
174B ->196B	0.10925				
177B ->197B	-0.22936				
181B ->198B	0.19695				
183B ->199B	-0.16531				
186B ->200B	-0.12016				
187B ->198B	-0.11608				

Excited State 270:	1.000-A	5.8085 eV	213.45 nm	f=0.0342	<S**2>=0.000
171A ->195A	-0.13321				
177A ->197A	0.15739				
177A ->198A	-0.10177				
180A ->198A	-0.11093				
181A ->197A	-0.30973				
181A ->198A	0.42219				
181A ->199A	0.13669				
192A ->202A	-0.12035				
192A ->203A	0.17897				
171B ->195B	-0.13321				
177B ->197B	0.15740				
177B ->198B	-0.10176				
180B ->198B	-0.11094				
181B ->197B	-0.30974				
181B ->198B	0.42222				
181B ->199B	0.13669				
192B ->202B	-0.12035				
192B ->203B	0.17897				

Excited State 273:	1.000-A	5.8302 eV	212.66 nm	f=0.0955	<S**2>=0.000
169A ->195A	0.18624				
171A ->195A	0.18618				
177A ->197A	0.36444				
180A ->197A	0.13712				
186A ->201A	-0.14046				
189A ->203A	0.12336				

192A ->202A	0.14806					
192A ->203A	-0.21813					
192A ->206A	-0.14414					
193A ->208A	0.10326					
169B ->195B	0.18624					
171B ->195B	0.18618					
177B ->197B	0.36444					
180B ->197B	0.13712					
186B ->201B	-0.14046					
189B ->203B	0.12336					
192B ->202B	0.14805					
192B ->203B	-0.21812					
192B ->206B	-0.14414					
193B ->208B	0.10326					
Excited State 274:	1.000-A	5.8305 eV	212.65 nm	f=0.0269	<S**2>=0.000	
177A ->197A	0.11743					
185A ->201A	-0.10834					
186A ->200A	0.10043					
186A ->201A	0.33479					
187A ->201A	-0.14298					
189A ->202A	0.21829					
189A ->203A	-0.28204					
192A ->203A	-0.14360					
194A ->220A	0.11901					
194A ->222A	-0.14291					
177B ->197B	0.11743					
185B ->201B	-0.10834					
186B ->200B	0.10043					
186B ->201B	0.33479					
187B ->201B	-0.14298					
189B ->202B	0.21829					
189B ->203B	-0.28204					
192B ->203B	-0.14360					
194B ->220B	0.11902					
194B ->222B	-0.14291					

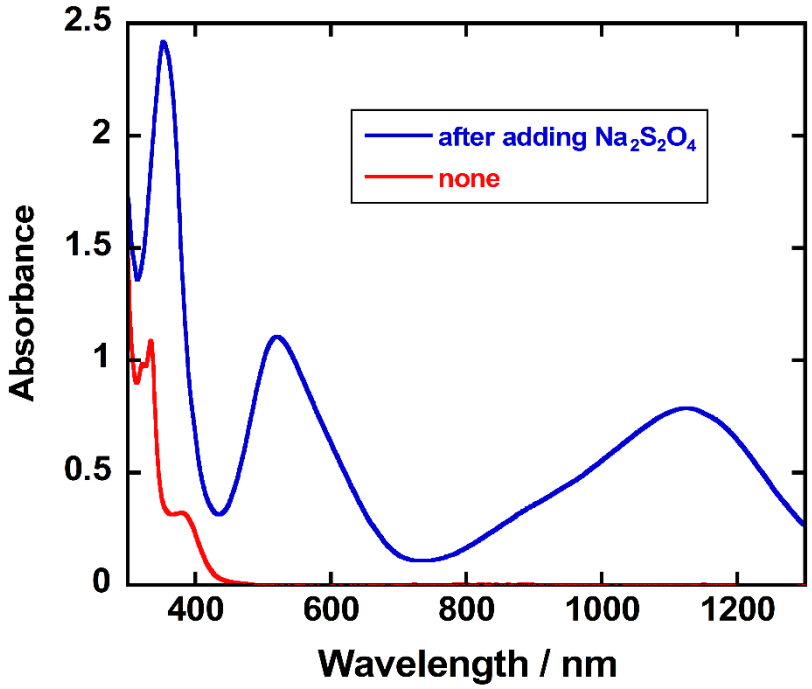

Fig. S6 A spectral change of an aqueous acetate buffer solution (pH 5.0; at 20 °C under Ar) containing 0.1 mM **[PtCl$_2$(bpyMV2)]$^{4+}$**, 0.1 M NaCl, and 30 mM EDTA by adding ca. 0.24 mg (1.38 μmol) of $Na_2S_2O_4$.

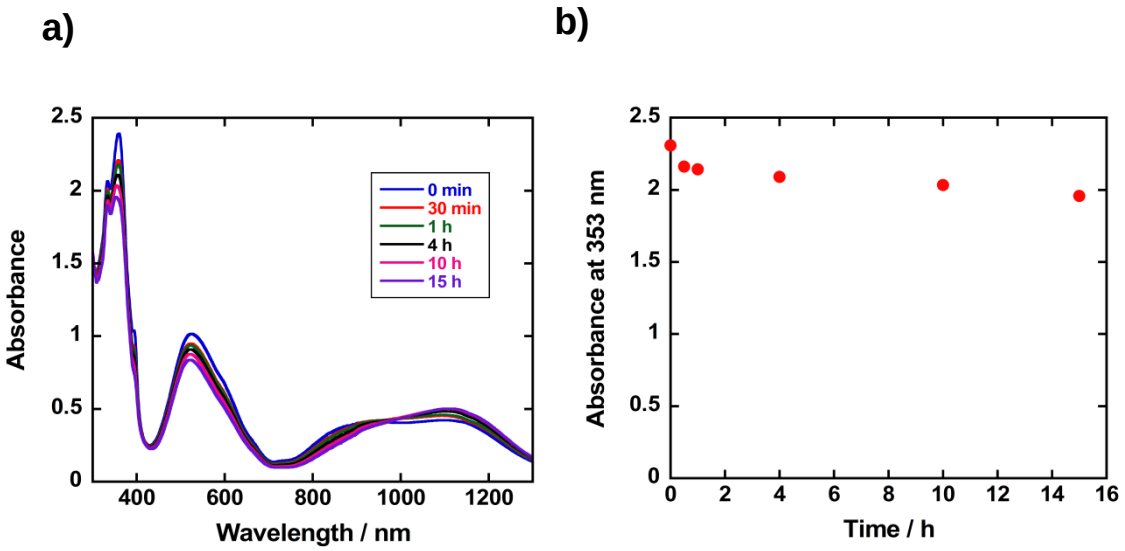

Fig. S7 a) Spectral changes observed for an aqueous acetate buffer solution (pH 5.0; at 20 °C under Ar) containing 0.1 mM **[PtCl$_2$(bpyMV2)]$^{4+}$**, 0.1 M NaCl, and 30 mM EDTA in the dark after visible light irradiation ($400 < \lambda < 800$ nm) for 10 min. b) Change in absorbance at 353 nm, taken from the spectral changes in Fig. S7a.

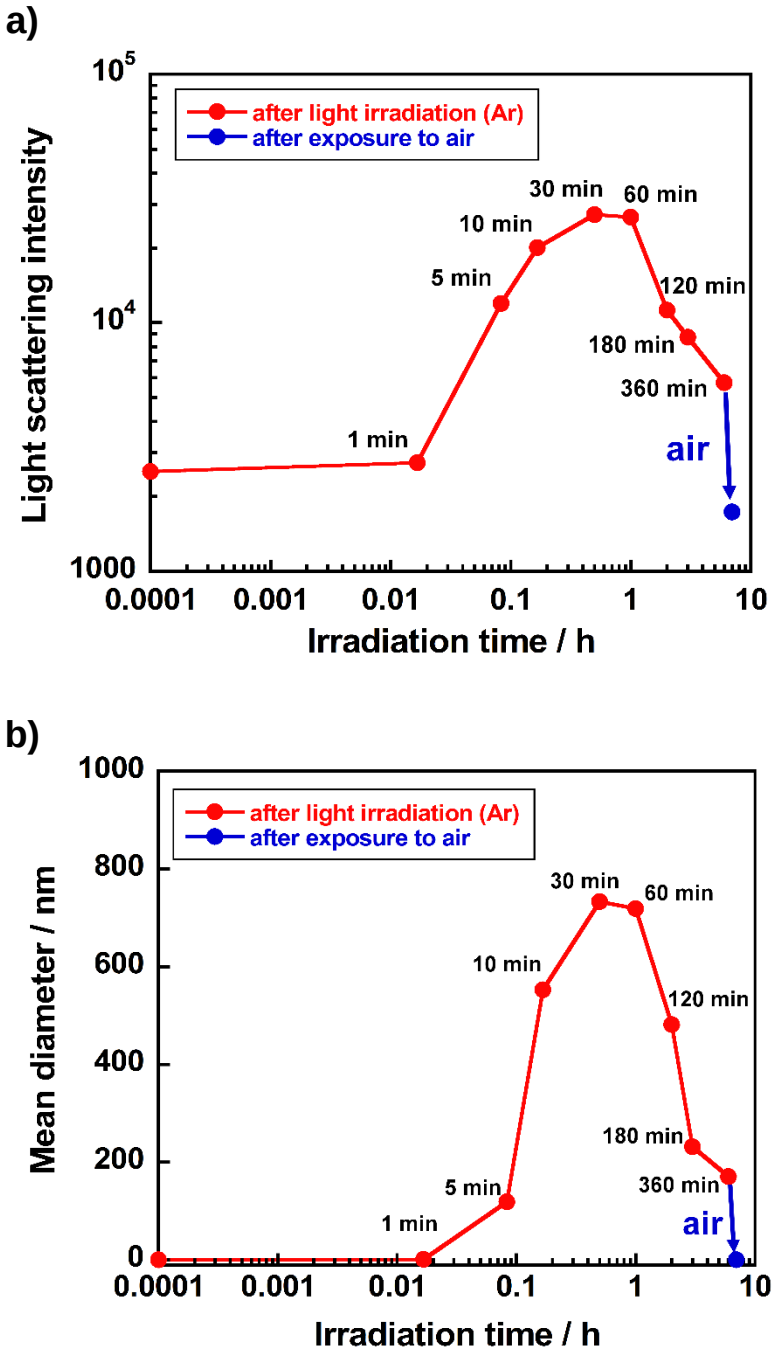

Fig. S8 DLS measurements during the photolysis of an aqueous acetate buffer solution (pH 5.0; at 20 °C under Ar) containing 0.1 mM **[PtCl$_2$(bpyMV2)]$^{4+}$**, 0.1 M NaCl, and 30 mM EDTA. a) Changes in light scattering intensity during the photolysis. b) Changes in a mean diameter of particles dispersed during the photolysis. The maximum particle size seen here (ca. 800 nm) is much larger than those of the platinum nanoparticles given from K_2PtCl_4 under similar experimental conditions (ca. 200 nm; data not shown).

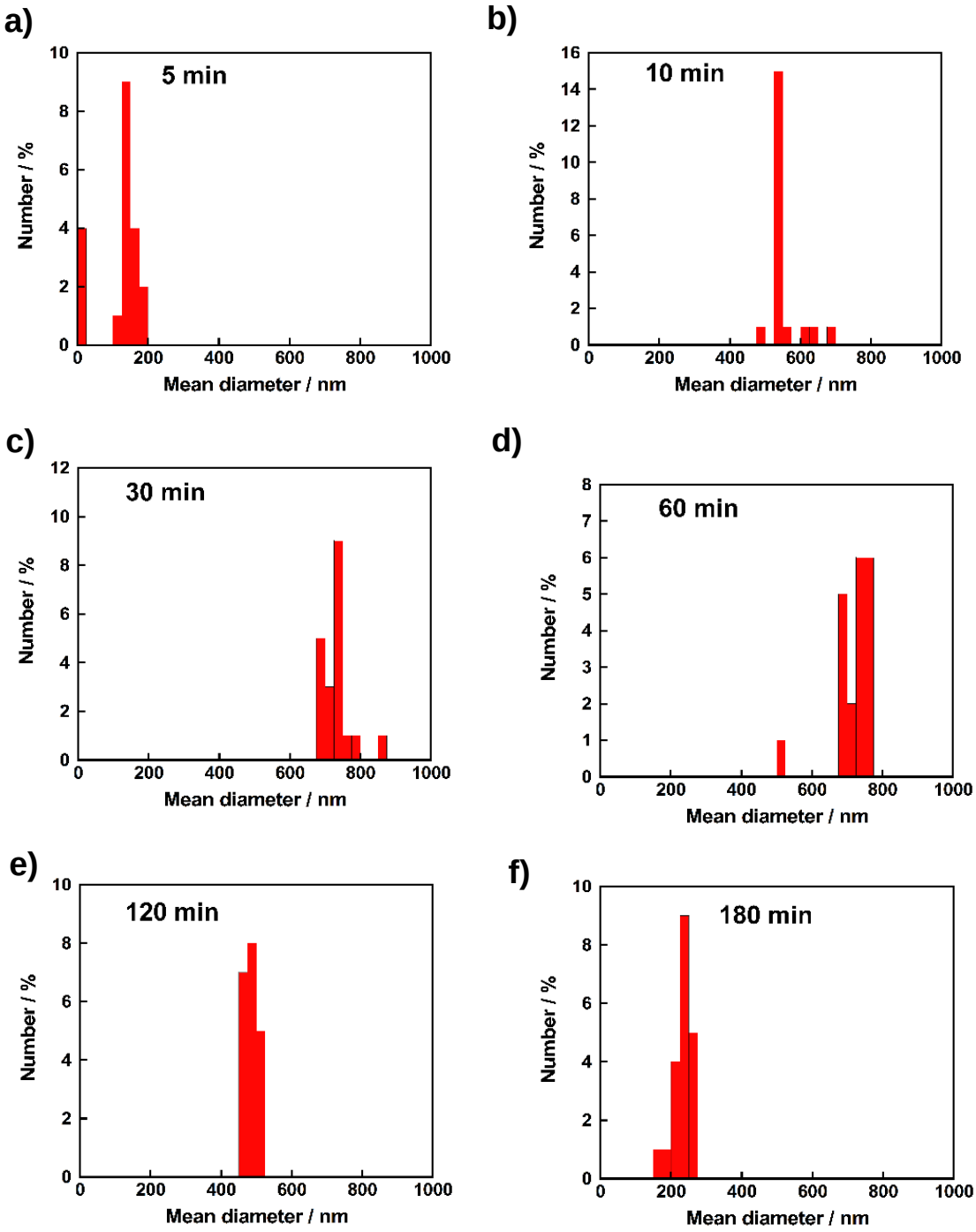

Fig. S9 The particle size distribution of unidentified particles generated during the photolysis experiments shown in Fig. S8 at a) 5 min, b) 10 min, c) 30 min, d) 60 min, e) 120 min, and f) 180 min.

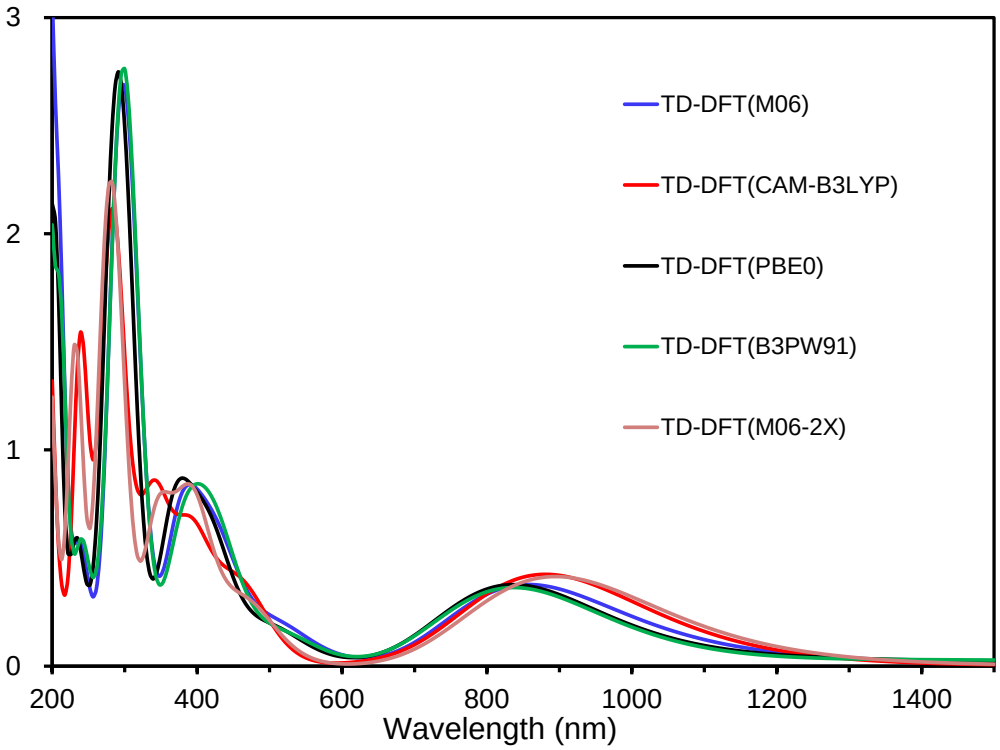

Fig. S10 Spectral features simulated based on the TD-DFT calculations using several different functionals, such as M06, CAM-B3LYP, PBE0, P3PW91, and M06-2X, where the structure of **$[PtCl_2(bpy)\text{-}(MV^+)_2]^{2+}$** (closed-shell singlet) employed was that optimized at the M06/SDD(Pt)/6-31G**(HCNOCl)/PCM level of DFT. The results given for the open-shell singlet states were identical to those given for the corresponding closed-shell singlet states and have been thereby omitted in this figure.

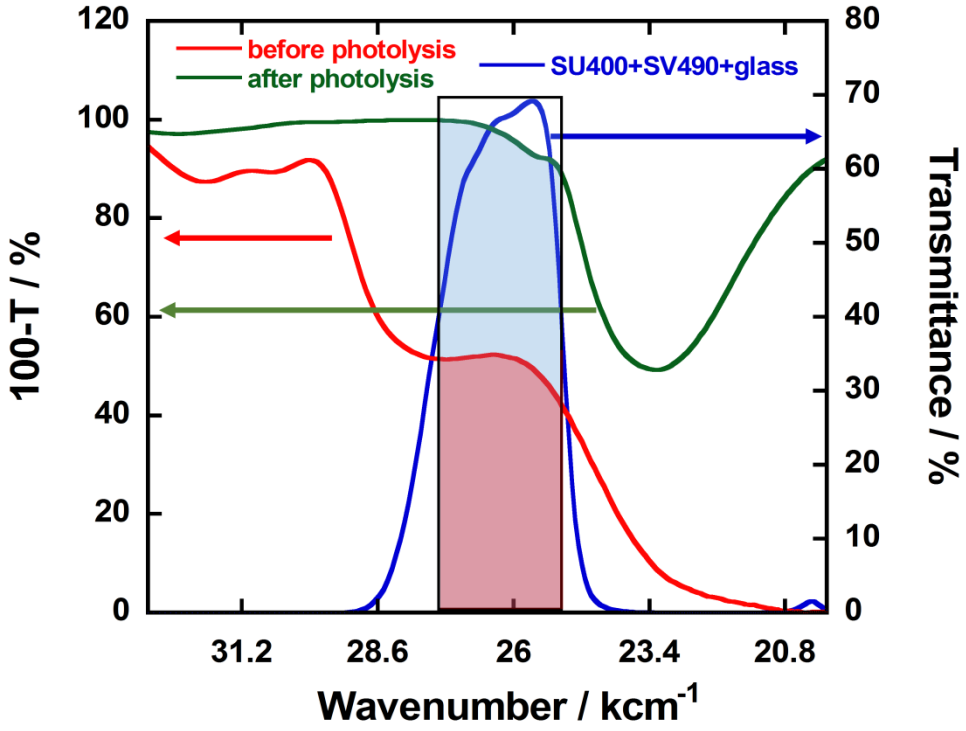

Fig. S11 Transmittance property for the employed combination of glass filters is shown by a blue line (this include the transmittance component of the Pyrex glass vial employed in the measurement). The red and green lines correspond to the absorption properties of non-reduced and two-electron-reduced species. With this feature, it was estimated that 53% of the incident light absorbed by the two-electron-reduced species contribute to the excitation of the $PtCl_2$(bpy)-based MLCT chromophore. As a result, the apparent quantum yield of H_2 formation was corrected by dividing it by this factor (i.e., 0.53).

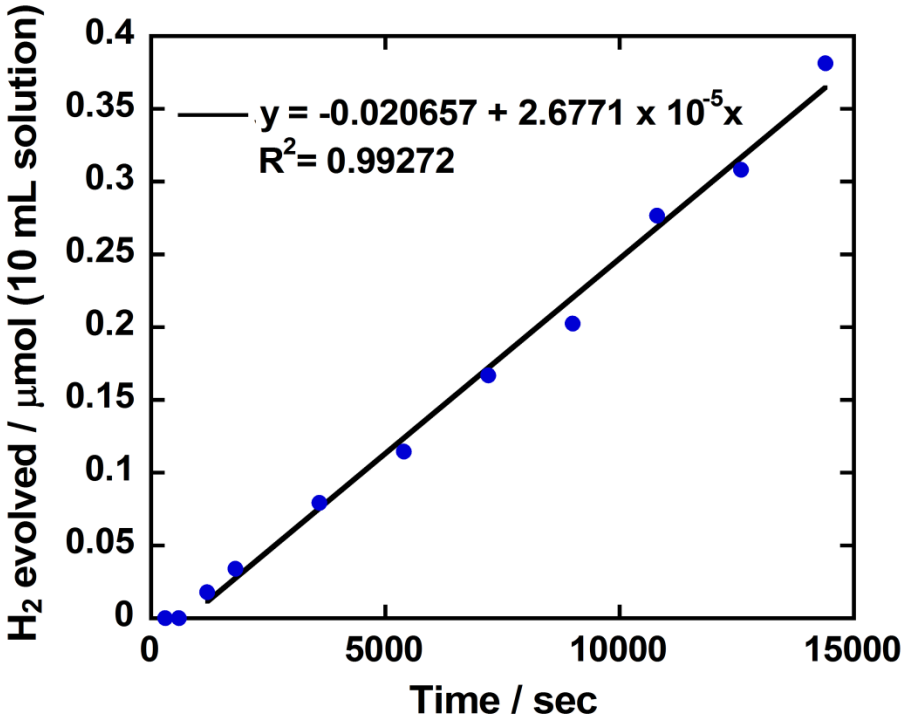

Fig. S12 Photochemical H_2 production from an aqueous acetate buffer solution (pH 5.0, 10 mL; at 20 °C under Ar) containing 0.1 mM **$[PtCl_2(bpyMV2)]^{4+}$**, 0.1 M NaCl, and 30 mM EDTA, under photoirradiation in the 360-400 nm domain using the set of glass filters described in Fig. S11.

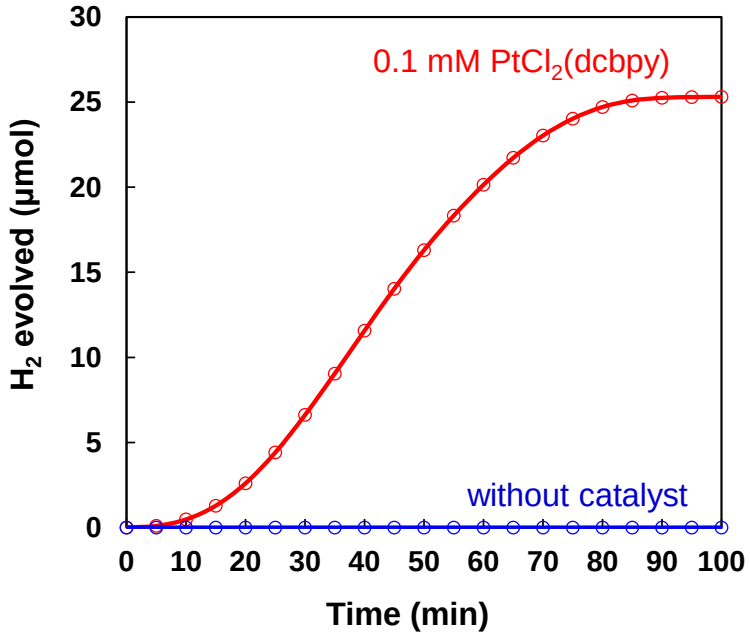

Fig. S13 Thermal hydrogen production after mixing $MV^{+\bullet}$ (68 μmol; 1.5 mM) with $PtCl_2$(dcbpy) (4.5 μmol; 0.1 mM) in an aqueous acetate buffer solutions containing 0.03 M CH_3COOH, 0.07 M CH_3COONa, and 0.1 M NaCl (pH 5.0, 45 mL) at 20 °C under Ar atmosphere. The solution of $MV^{+\bullet}$ was prepared by a bulk electrolysis of a solution of 5.0 mM $[MV]Cl_2 \cdot 3H_2O$ in the same buffer solution at –0.9 V vs. SCE. These experiments were performed as previously described.[S20]

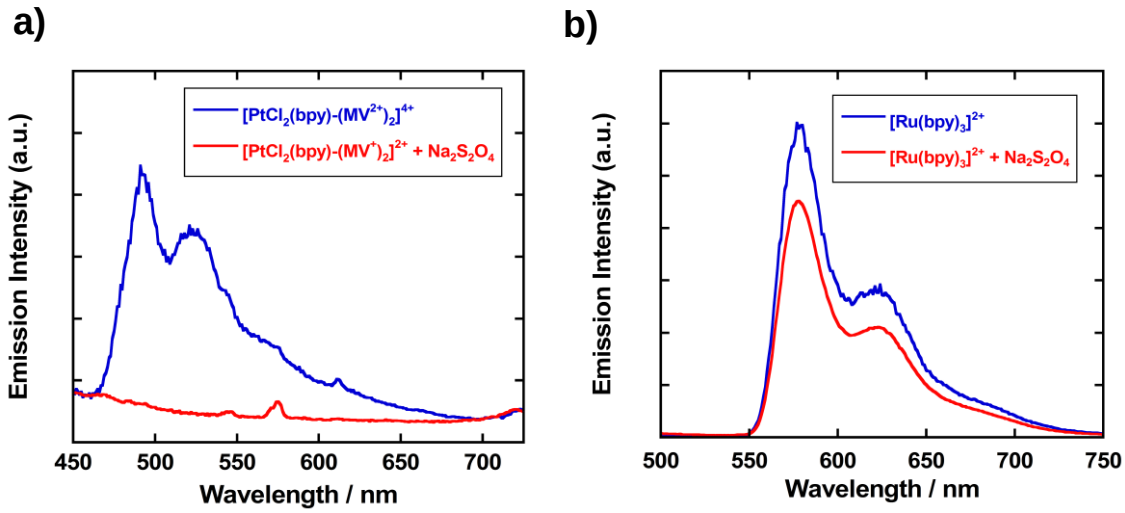

Fig. S14 a) Emission spectra (excitation at 380 nm) of the non-reduced species **$[PtCl_2(bpy)\text{-}(MV^{2+})_2]^{4+}$** (blue line) and the two-electron-reduced species **$[PtCl_2(bpy)\text{-}(MV^{+})_2]^{2+}$** (red line) generated by adding an excess of $Na_2S_2O_4$. The solution was prepared by dissolving the compound (0.01 mM) in a 1:2 mixture of aqueous acetate buffer (0.1 M, pH 5.0) containing NaCl (0.1 M) and ethylene glycol (0.25 mL) and was sealed in a quartz EPR tube under He. Measurements were carried out at 77 K in a frozen glass, before and after adding $Na_2S_2O_4$ (7 mg, 40 μmol). b) Emission spectra (excitation at 425 nm) of 0.01 mM $[Ru(bpy)_3](NO_3)_2 \cdot 3H_2O$ before (blue line) and after (red line) adding $Na_2S_2O_4$. The solution was prepared by dissolving the compound in a 1:2 mixture of water and ethylene glycol (0.25 mL) and was sealed in a quartz EPR tube under He. Other conditions are same to those described above. Note that the emission intensity was quite sensitive to the manually tuned position of each sample so that quantitative comparison of the emission intensities does not make sense. Judging from the results in Fig. S14b, we rule out the quenching of a ^{3}MLCT state by the presence of $Na_2S_2O_4$, leading to our conclusion that the ^{3}MLCT state generated within the two-electron-reduced species **$[PtCl_2(bpy)\text{-}(MV^{+})_2]^{2+}$** is effectively self-quenched by the $(MV^+)_2$ π-dimer unit tethered to the $PtCl_2$(bpy) moiety in a close contact.

References

[S1] A. R. Oki and R. J. Morgan, *Synth. Commun.*, 1995, **25**, 4093.

[S2] L. A. Kelly, and M. A. J. Rodgers, *J. Phys. Chem.*, 1994, **98**, 6386.

[S3] J. H. Price, A. N. Williamson, R. F. Schramm and B. B. Wayland, *Inorg. Chem.*, 1972, **11**, 1280.

[S4] H. Ozawa, M. Haga, and K. Sakai, *J. Am. Chem. Soc.*, 2006, **128**, 4926.

[S5] K. Sakai, Y. Kizaki, T. Tsubomura and K. Matumoto, *J. Mol. Catal.*, 1993, **79**, 141.

[S6] M. Kobayashi, S. Masaoka and K. Sakai, *Dalton Trans.*, 2012, **41**, 4903.

[S7] M. J. Frisch *et al*., Gaussian 09 Revision C.01 (Gaussian Inc., Wallingford CT, 2009).

[S8] Y. Zhao and D. G. Truhlar, *Theor. Chem. Acc.*, 2008, **120**, 215.

[S9] Y. Zhao and D. G. Truhlar, *J. Phys. Chem. A*, 2008, **112**, 1095.

[S10] Y. Zhao and D. G. Truhlar, *Acc. Chem. Res.*, 2008, **41**, 157.

[S11] V. Barone, M. Cossi and J. Tomasi, *J. Comp. Chem.*, 1998, **19**, 404.

[S12] M. Cossi, G. Scalmani, N. Rega and V. Barone, *J. Chem. Phys.*, 2002, **117**, 43.

[S13] J. Tomasi, B. Mennucci and R. Cammi, *Chem. Rev.*, 2005, **105**, 2999.

[S14] M. E. Casida, C. Jamorski, K. C. Casida and D. R. Salahub, *J. Chem. Phys*., 1998, **108**, 4439.

[S15] R. E. Stratmann, G. E. Scuseria and M. J. Frisch, *J. Chem. Phys.*, 1998, **109**, 8218.

[S16] R. Bauernschmitt and R. Ahlrichs, *Chem. Phys. Lett.*, 1996, **256**, 454.

[S17] GaussView, Version 5, R. Dennington, T. Keith and J. Millam, *Semichem Inc.*, Shawnee Mission, KS, 2009.

[S18] C. G. Hatchard and C. A. Parker, *Proc. R. Soc. London, Ser. A.*, 1956, **235**, 518-536.

[S19] D. R. James, Y.-S. Liu, P. De Mayo and W. R. Ware, *Chem. Phys. Lett.*, **1985**, *120*, 460-465.

[S20] K. Yamauchi, S. Masaoka, and K. Sakai, *J. Am. Chem. Soc.*, **2009**, *131*, 8404-8406.